Int. J. Electrochem. Sci., 16 **(2021)** Article ID: 210431, doi: 10.20964/2021.04.32

International Journal of ELECTROCHEMICAL SCIENCE
www.electrochemsci.org

Synthesis and characterization of NiS Nanoparticles@Carbon Nanofiber Composite as Electrocatalyst for Methanol Oxidation

Ibrahim M. Maafa

Chemical Engineering Department, College of Engineering, Jazan University, Jazan 45142, Saudi Arabia.
E-mail: imoaafa@jazanu.edu.sa

Received: 4 December 2020 / *Accepted:* 21 January 2021 / *Published:* 28 February 2021

This study aimed at the successful synthesis of NiS nanoparticle-decorated carbon nanofibers (NiS NPs/CNFs) by the electrospinning technique and their use as an electrocatalyst for methanol oxidation. NFs were prepared from calcination of electrospun nanofiber mats composed of polyvinyl pyrrolidone, nickel acetate tetrahydrate, and ammonium sulfide at 800 °C in inert atmosphere for 5 h. Standard characterization techniques (SEM, XRD, TEM, and TEM-EDX) showed the formation of nickel sulphide and carbon. The NiS NPs/CNFs prepared showed a good electrocatalytic activity toward methanol oxidation in alkaline media. The current density obtained was 20 $mAcm^{-2}$ at 4M methanol in 1M KOH solution. The NiS NPs/CNFs showed a good stability for 3000 s used in chronoamperometry test.

Keywords: Nickel sulphide; Carbon Nanofibers; Electrospinning; Electrooxidation; Methanol

1. INTRODUCTION

Besides its expected depletion, fossil fuel has a serious effect on environment and human health, as it causes the green-house effect[1]. This has led researchers to seek sustainable, low cost and environment-friendly sources of energy (e.g. wind energy, waterfalls, photovoltaic cells, and fuel cells (FCs). FCs are electrochemical devices that convert the energy of a chemical reaction directly into electrical energy and produce water as by-product [2, 3]. Among FCs, direct methanol fuel cells (DMFCs) use methanol (MeOH) as a fuel, which has wide application, including in electric vehicles and mobile systems [4, 5]. MeOH is directly converted into electricity by an electrochemical reaction and the production of carbon dioxide and water. DMFCs can be operated at room temperature with high efficiency. DMFCs have various applications as in portable power sources, electric vehicles and transport. Catalysts are considered the key factor in the methanol oxidation performance. Pt-based electrocatalysts are the most active ones for alcohol oxidation reaction [6-8]. However, the high cost of

platinum, besides its low availability and serious surface poisoning by CO species resulting in blocking the active electrocatalyst sites, limits its wide application. These drawbacks have prompted many researchers to examine cheap and active transition metals (TMs), transition metal carbides (TMCs), transition metal phospides (TMPs), and transition metal suphides (TMSs) as alternative electrocatalysts [9-11]. Nickel Sulfide (NiS) [12, 13] is amongst the TMSs synthesized as catalysts and electrocatalysts in energy-based devices in recent years. It is applied in different chemical reactions and energy-based devices [11]. Carbon nanostructures show a distinct impact on the physical and chemical properties of the incorporated catalysts and electrocatalysts material; accordingly, the catalytic and electrocatalytic activity will be strongly modified [14-16]. Herein, NiS nanoparticles/carbon nanofibers (NiS NPs/CNFs) were prepared from a solution consisting of nickel acetate tetrahydrate and Polyvinylpyrrolidone using *in situ* sulfurization, electrospinning, and calcination processes. The synthesized nanofibers displayed a good electrocatalytic performance in methanol oxidation in alkaline media.

2. EXPERIMENTAL SECTION

2.1. Materials

Nickel acetate tetrahydrate (NiAc), ammonium sulfide (NH_4S), polyvinylpyrrolidone (PVP, average molecular weight~1300 kg mol-1), methanol (MeOH) and ethanol were purchased from Sigma-Aldrich.

2.2. Preparation of NiS NPs/CNFs

PVP powder was dissolved into ethanol solution to prepare 15 wt % PVP. 20 wt% nickel acetate tetrahydrate–based PVP was added to aforementioned solution. The mixture formed was kept in the stirrer at 60 °C for 5 h to obtain homogeneous and clear sol-gel. Colloidal solution was obtained after addition of dropwise from NH_4S to the previous sol-gel. This solution was electrospun using lab-scale electrospinning equipment. Typically, the solution was poured into a 10 ml plastic syringe. 20 kV potential was applied and 20 cm distance maintained between the stainless-steel needle and rotating stainless-steel cylinder covered with aluminum foil. The electrospun NF mats produced were dried under vacuum at 50 °C for 24 h and sintered at 800 °C under Ar atmosphere for 5 h, for obtaining NiS NPs/CNFs.

2.3. Electrode preparation and electrochemical measurements

The electrocatalytic performance of NiS NPs/CNFs was accomplished by three-electrode electrochemical cell system. NiS NPs/CNFs, platinum rod, and Ag/AgCl (3M KCl) were applied as working electrode, counter electrode, and reference electrode, respectively. 2 mg from synthesized nanofibers was mixed with 20 μL Nafion solution (5 wt%) and 400 μL isopropanol. 15 μL from the

prepared slurry was poured on the glassy carbon electrode (GCE). Electrode was dried at 80 °C for 10 min. Cyclic voltammetry test (CV) was used to determine the electro-catalytic activity of NiS NPs/CNFs. The study achieved 1M KOH solution and different concentrations of MeOH with sweep potential ranging from 0 to 0.8 V. Chronoamperometery test (CA) of synthesized NFs was done at 0.45 V. Electrochemical impedance spectroscopy measurements (EIS) were carried out at constant dc potential, 10 mV amplitude ac voltage, and frequency range of 1×10^{-4} – 0.1 Hz.

2.4. Characterization

Scanning electron microscope (SEM, Hitachi S-7400, Japan) was used to observe the morphology of the nanofibers prepared. The microscope was a transmission electron microscope (TEM) (JEOL Ltd., Japan) equipped with EDX for the investigation of the crystallinity of nanocomposite. X-ray diffraction technique with Cu Kα (λ=1.54056 Å) (Rigaku Co., Japan) was used to determine the crystallinity structure of nanocomposite.

3. RESULTS AND DISCUSSION

3.1. Characterization

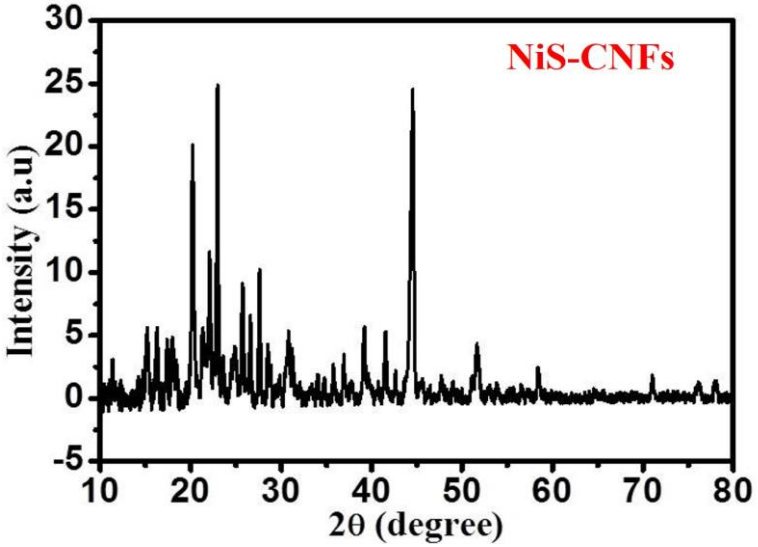

Figure 1. XRD of NiS NPs/CNFs powder obtained after calcination.

Figure 1 shows the XRD pattern of the synthesized NiS NPs/CNFs. Two peaks appeared at 23.5° and 44.3° and agreed well with carbon peaks, as described in the literature [17, 18]. The additional peaks are well consistent with NiS (JCPDS = 73-0574) [19-21]. Barakat et al [22-24], indicated the formation of carbon nanofibers from different types of polymers during heat treatment in inert gas, in the presence of Ni and Ni-based materials. Further, they obtained well-attached nanoparticles inside and/or attached the surface carbon nanofibers, when the electrospunnano fiber

mats from different colloidal solutions were calcined. SEM image (Figure 2A) shows a good nanofibrous morphology without beads after calcination at 800 °C under Ar atmosphere for 5 h. To get a visible morphology of NF structure, STEM image of one NF is presented in Figure 2B. As seen in the Figure, clear white NPs are grown and encapsulated into NFs.

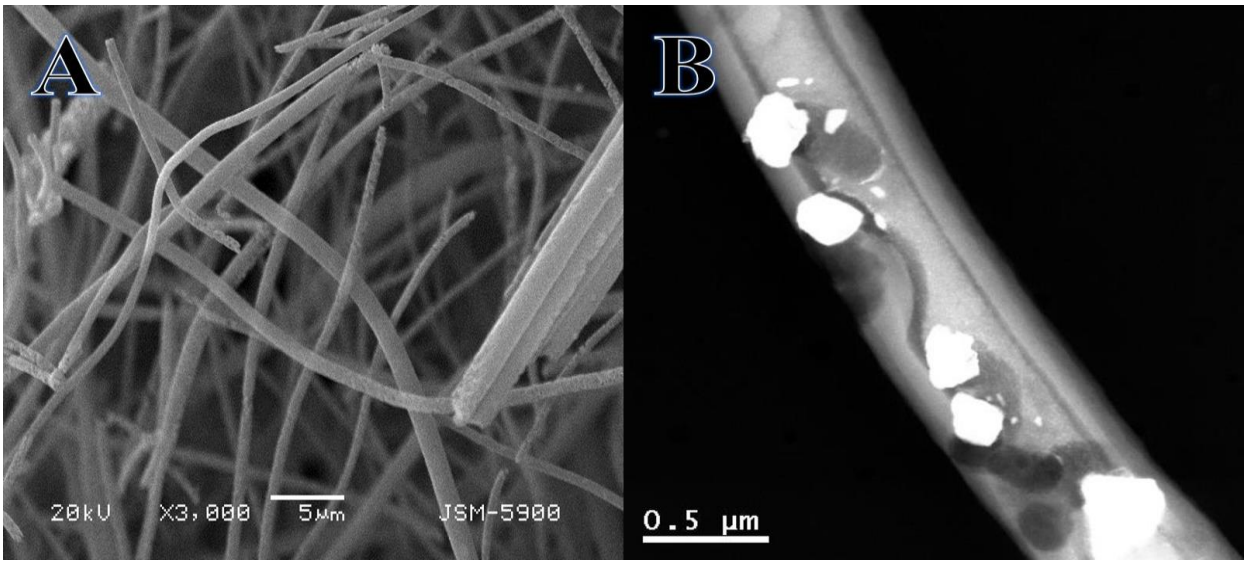

Figure 2. FE-SEM and STEM images of NiS NPs/CNFs powder produced after calcination.

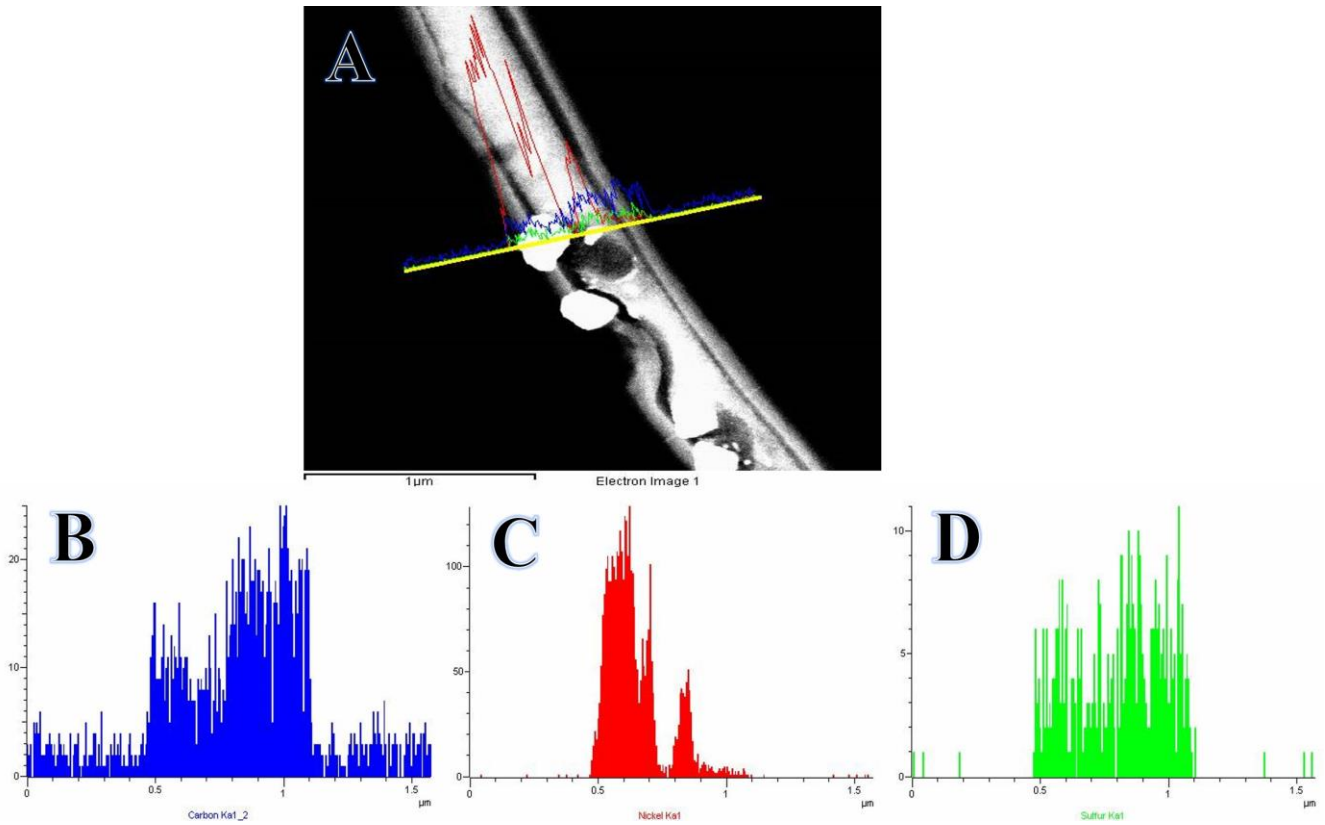

Figure 3. A) STEM image of a single NF and B-D) TEM-EDX analysis of the powder produced after calcination.

To obtain the elemental analysis of the fabricated NFs, TEM-EDX analysis was used. TEM-EDX spectrum (Figure 3C, D and E) was corresponding to the line shown in Figure 3A. Figure 3C and D revealed that the nickel and sulphur have a uniform distribution along the selected line, suggesting the formation of nickel sulphide NPs. Carbon is shown as the outer most element (Figure 3D). In other words, carbon nanofibers are well enveloped in the nickel sulphide NPs, which is clear at all points along with the selected line. This is confirmed by the XRD analysis about the formation of nickel sulphide and carbon. Carbon has a high adsorption capacity and chemical stability. The carbon nanofibers produced used an electrospinning technique having a nanoporous structure, which could be enhanced by the electrocatalytic activity [25].

3.2. Electrochemistry study

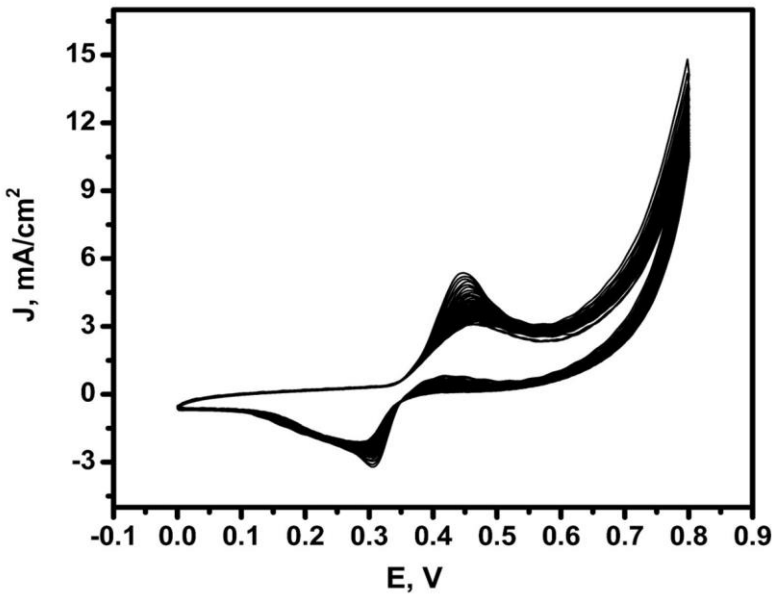

Figure 4. CV for the activation of NiS NPs/CNFs in 1M KOH at 50 mV/s.

The electrocatalytic performance of NiS NPs/CNFs made as anode towards MeOH oxidation reaction was measured by CV, EIS, and CA techniques. Nickel and nickel-based electrocatalyst materials should be sweeping in an alkaline medium to form an active layer, before being used in MeOH Oxidation reaction [26-28]. The CV behavior of NiS NPs/CNFs in 1M KOH solution at 50 mV/s for 50 cycles within a potential window of 0 to 0.8 V (vs. Ag/AgCl) (

Figure 4). Two redox peaks were observed at potential values of 0.30 V and 0.45 V for oxidation and reduction peaks, respectively. The first peak represents the nickel oxidation according to the following reaction:

$Ni+2OH^- \rightarrow NiOOH + H_2O + 2e^-$ (1)

Usually, the aforementioned peak is small in the first cycle and more decrease was observed in the consequent ones [28-31]. The second peak can be seen in the positive potential region; this peak was ascribed the $Ni(OH)_2$/NiOOH transformation [30, 32, 33]:

$$Ni(OH)_2 + OH^- \rightarrow NiOOH + H_2O + e^- \quad (2)$$

The peaks' current density increased with increase in the number of cycles up to the completion of the activation process (formation of NiOOH); this is due to the built in of OH^- into the $Ni(OH)_2$ surface layer; which led to the increase of the layer thickness of NiOOH after several consecutive CV cycles. However, further increase in NiOOH layer is not desirable in MeOH oxidation, because the resistance of the electrode is increased [34, 35]. Indeed, the electrooxidation of Ni working electrodes at high pH was carried out in two steps, started by the formation of $Ni(OH)_2$ from Ni [36-38]. There are two forms $Ni(OH)_2$: α- $Ni(OH)_2$ and β- $Ni(OH)_2$. β- $Ni(OH)_2$ could be oxidized to β-NiOOH, which would be γ-NiOOH and accumulated at the working electrode surface [38, 39]. In short, the NiS NPs/CNFs working electrode is electroactive and can form NiOOH, which is the electroactive layer for electrocatalytic processes like MeOH oxidation.

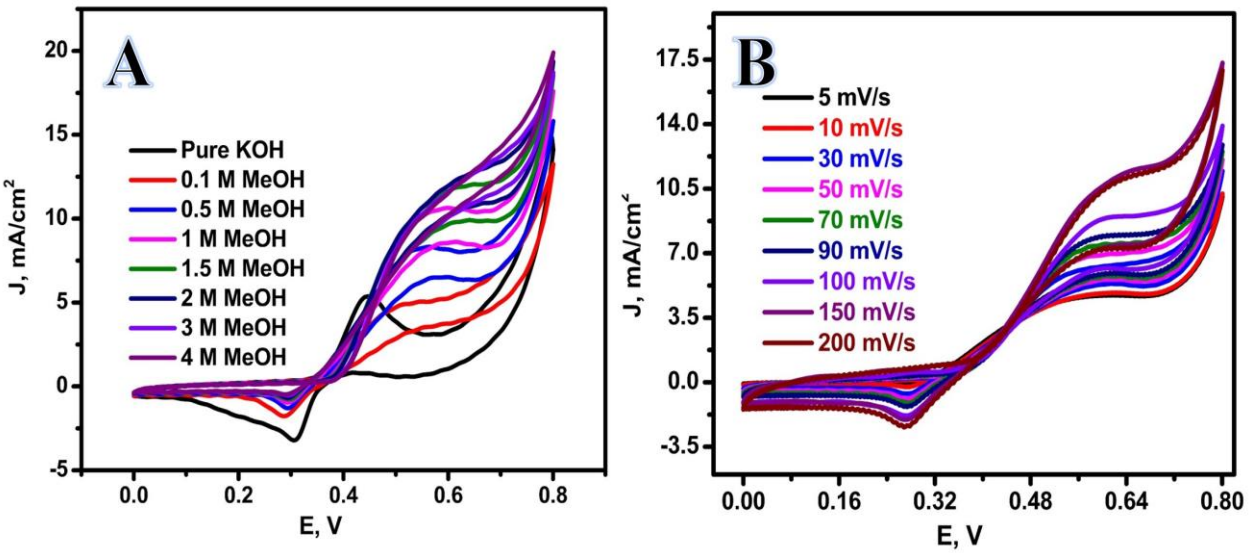

Figure 5. CV of the NFs prepared in the presence of different concentrations from MeOH (A) and different scan rates (B).

Figure 5A reveals the effect of increase MeOH concentration from 0.1M to 4M on the current density using NiS NPs/CNFs electrode at 50 mV/s within a potential window of 0 to 0.8 V. The oxidation of MeOH molecules happens at a higher potential than the oxidation of $Ni(OH)_2$/NiOOH[40]. Increasing MeOH concentration on the supporting electrolyte resulted in increase in the current density, which showed MeOH oxidation on the NiOOH layer (equ. 3)[40] at a potential value of 0.6 V. The enhancement of oxidation or anodic peak with the increase of MeOH concentration can be a solid proof of the high performance of the NiS NPs/CNFs electrode utilized as an electrocatalyst for MeOH oxidation.

$$NiOOH + MeOH \rightarrow Ni(OH)_2 + product \quad (3)$$

The highest oxidation current density (20 $mA.cm^{-2}$) was obtained at 4M MeOH. The good electrocatalytic performance resulted from nanofiberous morphology, which enhances the electron

transport through electrocatalyst. The composite NFs prepared have been compared with the different Ni- based catalysts in the MeOH electro-oxidation (Table 1).

Table 1. The electrocataytic activity of various Ni-based catalysts towards MeOH oxidation.

Catalyst	MeOH (M)	Electrolyte Support	I (mA. cm^{-2})	Scan Rate ($mV.s^{-1}$)	Ref.
$NiCo_2O_4$NPs/rGO	0.5	1 M KOH	16.6	50	[41]
$NiCo_2O_4$ nanosheets	0.5	0.1 M KOH	14	50	[42]
Ni_2Cr_1NPs	1	0.25 M NaOH	16	100	[43]
NiCoCuNPs	0.5	0.1 M NaOH	20	100	[44]
Ni-Cu-P	0.5	0.1 M KOH	17	10	[45]
Ni-P/RGO	0.5	1 M KOH	16.4	10	[46]
NiS NPs/CNFs	4	1 M KOH	20	50	This Study

The effect of varying the scan rate (5,10, 30, 50, 70, 90, 100, 150, 200 mV/s) on the electrocatalytic performance of NiS NPs/CNFs for MeOH oxidation is shown in Figure 5B. The densities of both anodic and cathodic peak current are increased with the increase in the scan rate; the corresponding potential shifts towards more positive and negative values, respectively. This indicates MeOH oxidation occurring as follows (i) the fast electrosporption of MeOH molecules, (ii) fragmentation of MeOH into intermediates on the active surface sites; (iii) oxidation products obtained [32].

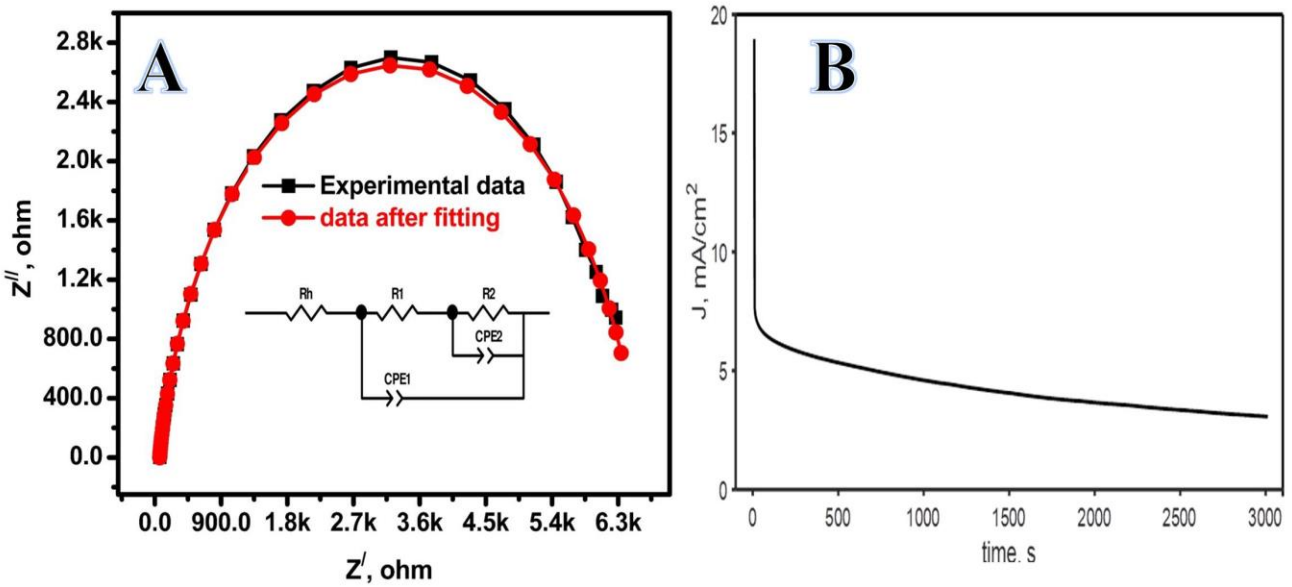

Figure 6. Nyquist plot (A) and Chronoamperogram of MeOH oxidation at NiS NPs/CNFs (B).

Figure 6A illustrates the characteristics of the electrochemical impedance spectroscopy (EIS) by the use of NiS NPs/CNFs electrode in the presence of MeOH and KOH solution. It has the EIS data before and after fitting by the use of an equivalent circuit, which is displayed in the inset of Figure 6A. The fitted EIS data were close to the experimental one, which indicates the successful fitting by the equivalent circuit utilized. The Nyquist ($Z^{/}$, $-Z^{//}$) data displayed only one semicircle, which could be assigned to the electrooxidation of MeOH. The presence of only one semicircle can be due to the interaction between the two charge transfer processes, viz., the formation of NiOOH and direct MeOH oxidation. It could be expected that both the indirect and direct electrooxidation reactions exist on the NiS NPs/CNFs electrode [47].

The long-term stability of NiS NPs/ CNFs electrode was evaluated using chronoamperometry with the constant potential value of 500 mV (Ag/AgCl) for a duration of 3000 s in 1M KOH solution containing 4M methanol in Figure 6B. The test was achieved in 1M KOH solution containing 4M methanol at a constant potential step of 500 mV (Ag/AgCl) for a duration of 3000 s in Figure 6B. Current density decreased sharply, followed by a steady state behavior, due to the consumption of MeOH from the solution.

4. CONCLUSION

NiS NPs/CNFs have been successfully prepared using *in situ* sulfurization and electrospinning processes. The nanofibers prepared showed a good nanofibrous structure after calcination of electrospun nanofiber mats composed of polyvinylpyrrolidone, nickel acetate tetrahydrate, and ammonium sulfide at 800 °C in inert atmosphere for 5 h. Further, TEM-EDX showed that the NiS NPs are sheathed by layer from CNFs. The as-synthesized NiS NPs/CNFs showed a good electrocatalytic activity toward methanol oxidation in alkaline media. Overall, this study presented a cheap and effective electrocatalyst.

References

1. M.W. Ellis, M.R. Von Spakovsky and D.J. Nelson, *Proc. IEEE*, 89 (2001) 1808.
2. A.B. Stambouli and E. Traversa, *Renewable Sustainable Energy Rev.*, 6 (2002) 295.
3. C. Wang and M.H. Nehrir, Distributed generation applications of fuel cells, in: 2006 Power Systems Conference: Advanced Metering, Protection, Control, Communication, and Distributed Resources, *IEEE*, 2006, pp. 244.
4. C. Lamy, E. Belgsir and J. Leger, *J. Appl. Electrochem.*, 31 (2001) 799.
5. E. Peled, T. Duvdevani, A. Aharon and A. Melman, *Electrochemical and Solid State Letters*, 4 (2001) A38.
6. S. Chen and M. Schell, *J. Electroanal. Chem.*, 478 (1999) 108.
7. C. Xu, P.K. Shen, X. Ji, R. Zeng and Y. Liu, *Electrochem. Commun.*, 7 (2005) 1305.
8. Z. Wei, L. Li, Y. Luo, C. Yan, C. Sun, G. Yin and P. Shen, *The Journal of Physical Chemistry B*, 110 (2006) 26055.
9. X. Li, A.M. Elshahawy, C. Guan and J. Wang, *Small*, 13 (2017) 1701530.
10. Y.C. Kimmel, X. Xu, W. Yu, X. Yang and J.G. Chen, *ACS Catal.*, 4 (2014) 1558.
11. P. Geng, S. Zheng, H. Tang, R. Zhu, L. Zhang, S. Cao, H. Xue and H. Pang, *Adv. Energy Mater.*, 8 (2018) 1703259.
12. H. Emadi, M. Salavati-Niasari and A. Sobhani, *Adv. Colloid Interface Sci.*, 246 (2017) 52.
13. N.A. Dhas, A. Ekhtiarzadeh and K.S. Suslick, *J. Am. Chem. Soc.*, 123 (2001) 8310.
14. A. Yousef, R.M. Brooks, M.H. El-Newehy, S.S. Al-Deyab and H.Y. Kim, *Int. J. Hydrogen Energy*, 42 (2017) 10407.
15. A.M. Al-Enizi, R.M. Brooks, A. Abutaleb, M. El-Halwany, M.H. El-Newehy and A. Yousef, *Ceram. Int.*, 43 (2017) 15735.
16. A. Yousef, R.M. Brooks, M. El-Halwany, A. Abutaleb, M.H. El-Newehy, S.S. Al-Deyab and H.Y. Kim, *Mol. Catal.*, 434 (2017) 32.
17. J. Xu, L. Zhang, G. Xu, Z. Sun, C. Zhang, X. Ma, C. Qi, L. Zhang and D. Jia, *Appl. Surf. Sci.*, 434 (2018) 112.
18. A.D. Faisal and A.A. Aljubouri, *Int. J. Adv. Mat. Res.*, 2 (2016) 86.
19. H. Seyghalkar, M. Sabet and M. Salavati-Niasari, *High Temp. Mater. Processes*, 35 (2016) 1017.
20. L. Mi, Y. Chen, W. Wei, W. Chen, H. Hou and Z. Zheng, *RSC Adv.*, 3 (2013) 17431.
21. Y. Ji, W. Liu, Z. Zhang, Y. Wang, X. Zhao, B. Li, X. Wang, X. Liu, B. Liu and S. Feng, *RSC Adv.*, 7 (2017) 44289.
22. B.M. Thamer, M.H. El-Newehy, S.S. Al-Deyab, M.A. Abdelkareem, H.Y. Kim and N.A. Barakat, *Appl. Catal., A*, 498 (2015) 230.
23. N.A. Barakat, M. El-Newehy, S.S. Al-Deyab and H.Y. Kim, *Nanoscale Res. Lett.*, 9 (2014) 2.
24. A. Yousef, R.M. Brooks, M. El-Halwany, M.H. EL-Newehy, S.S. Al-Deyab and N.A. Barakat, *Ceram. Int.*, 42 (2016) 1507.
25. R. M Brooks, I.M. Maafa, A. M Al-Enizi, M. M El-Halwany, M. Ubaidullah and A. Yousef, *Nanomaterials*, 9 (2019) 1082.
26. M. Alajami, M.A. Yassin, Z.K. Ghouri, S. Al-Meer and N.A. Barakat, *Int. J. Hydrogen Energy*, 43 (2018) 5561.
27. N.A. Barakat, M.A. Abdelkareem, M. El-Newehy and H.Y. Kim, *Nanoscale Res. Lett.*, 8 (2013) 1.
28. N.A. Barakat, M.A. Yassin, F.S. Al-Mubaddel and M.T. Amen, *Appl. Catal., A*, 555 (2018) 148.
29. M.A. Rahim, R.A. Hameed and M. Khalil, *J. Power Sources*, 134 (2004) 160.
30. F. Hahn, B. Beden, M. Croissant and C. Lamy, *Electrochim. Acta*, 31 (1986) 335.
31. M. Vuković, *J. Appl. Electrochem.*, 24 (1994) 878.

32. M. Fleischmann, K. Korinek and D. Pletcher, *J. Electroanal. Chem. Interfacial Electrochem.*, 31 (1971) 39.
33. O. Enea, *Electrochim. Acta*, 35 (1990) 375.
34. I.G. Casella, M.R. Guascito and M.G. Sannazzaro, *J. Electroanal. Chem.*, 462 (1999) 202.
35. A. Yousef, R.M. Brooks, M.A. Abdelkareem, J.A. Khamaj, M. El-Halwany, N.A. Barakat, M.H. EL-Newehy and H.Y. Kim, *ECS Electrochemistry Letters*, 4 (2015) F51.
36. A. Van der Ven, D. Morgan, Y. Meng and G. Ceder, *J. Electrochem. Soc.*, 153 (2005) A210.
37. N.A. Barakat, M.H. El-Newehy, A.S. Yasin, Z.K. Ghouri and S.S. Al-Deyab, *Appl. Catal., A*, 510 (2016) 180.
38. H.M. Abd El-Lateef, N.F. Almulhim and I.M. Mohamed, *J. Mol. Liq.*, 297 (2020) 111737.
39. N.A. Barakat, M. Motlak, A.A. Elzatahry, K.A. Khalil and E.A. Abdelghani, *Int. J. Hydrogen Energy*, 39 (2014) 305.
40. R.A. Hameed, *Appl. Surf. Sci.*, 357 (2015) 417.
41. E. Umeshbabu and G.R. Rao, *Electrochim. Acta*, 213 (2016) 717.
42. P. Manivasakan, P. Ramasamy and J. Kim, *Nanoscale*, 6 (2014) 9665.
43. Y. Gu, J. Luo, Y. Liu, H. Yang, R. Ouyang and Y. Miao, *J. Nanosci. Nanotechnol.*, 15 (2015) 3743.
44. T. Rostami, M. Jafarian, S. Miandari, M.G. Mahjani and F. Gobal, *Chin. J. Catal.*, 36 (2015) 1867.
45. R.A. Hameed and K. El-Khatib, *Int. J. Hydrogen Energy*, 35 (2010) 2517.
46. H. Zhang, C.-D. Gu, M.-L. Huang, X.-L. Wang and J.-P. Tu, *Electrochem. Commun.*, 35 (2013) 108.
47. F. Guo, K. Ye, M. Du, X. Huang, K. Cheng, G. Wang and D. Cao, *Electrochim. Acta*, 210 (2016) 474.